

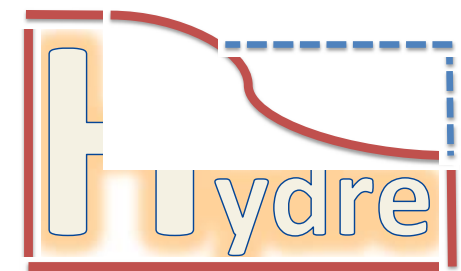


Projet ANR HYDRE

Anh Minh TANG

Ecole des Ponts ParisTech

Journée thématique SFT (22 janvier 2016)

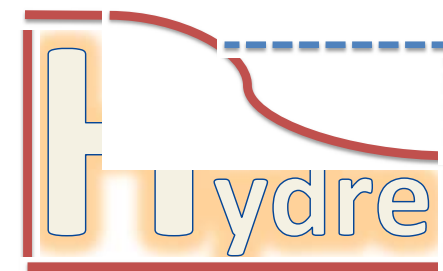


HYDRE

- Comportement mécanique des sédiments contenant des hydrates de gaz
- Partenaires:



- Début: 1^{er} novembre 2015
- Durée : 42 mois
- Aide ANR: 800 k€
- Coût complet: 2 500 k€

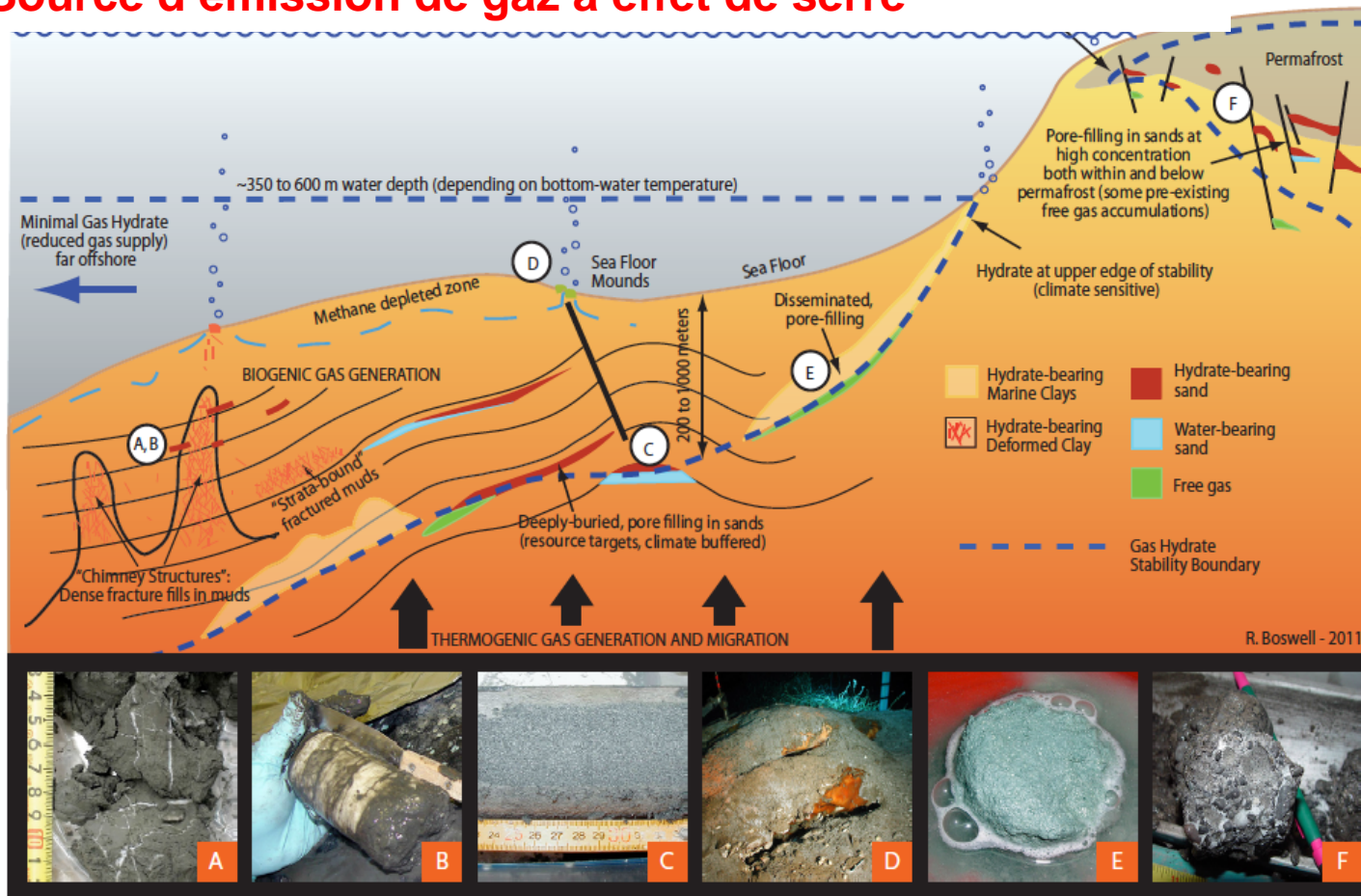


Contexte

Resource énergétique potentiellement importante

Source d'instabilité de talus continentaux

Source d'émission de gaz à effet de serre





Objectif

Etudier le comportement mécanique des sédiments contenant des hydrates de gaz afin de pouvoir réduire l'impact environnemental de leur potentielle exploitation future



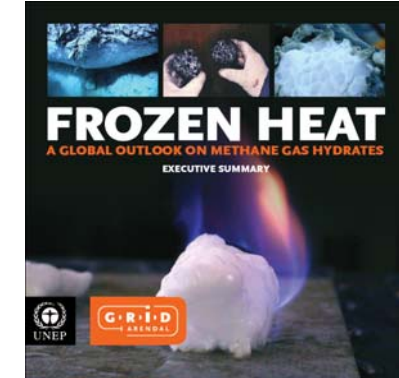
Verrous

Mécanismes de formation et de dissociation des hydrates dans les sédiments

Influence de la présence des hydrates sur le comportement mécanique des sédiments

Détection à partir des mesures in situ de la présence des hydrates

Adaptation des dispositifs expérimentaux existants aux conditions de haute pression et basse température nécessaires à la formation des hydrates



Etat de l'Art

Documentaire Arte (2014): Méthane, rêve ou cauchemar

COST MIGRATE (1405): Marine gas hydrate - an indigenous resource of natural gas for Europe

Norway: <http://www.cage.uit.no/>

Germany: <http://www.geomar.de/en/research/fb2/fb2-mg/projects/sugar-2-phase/>

Japan: <http://www.mh21japan.gr.jp/english/>

USA: <http://www.netl.doe.gov/research/oil-and-gas/methane-hydrates>

New Zealand: <http://www.gns.cri.nz/Home/Our-Science/Energy-Resources/Gas-Hydrates>

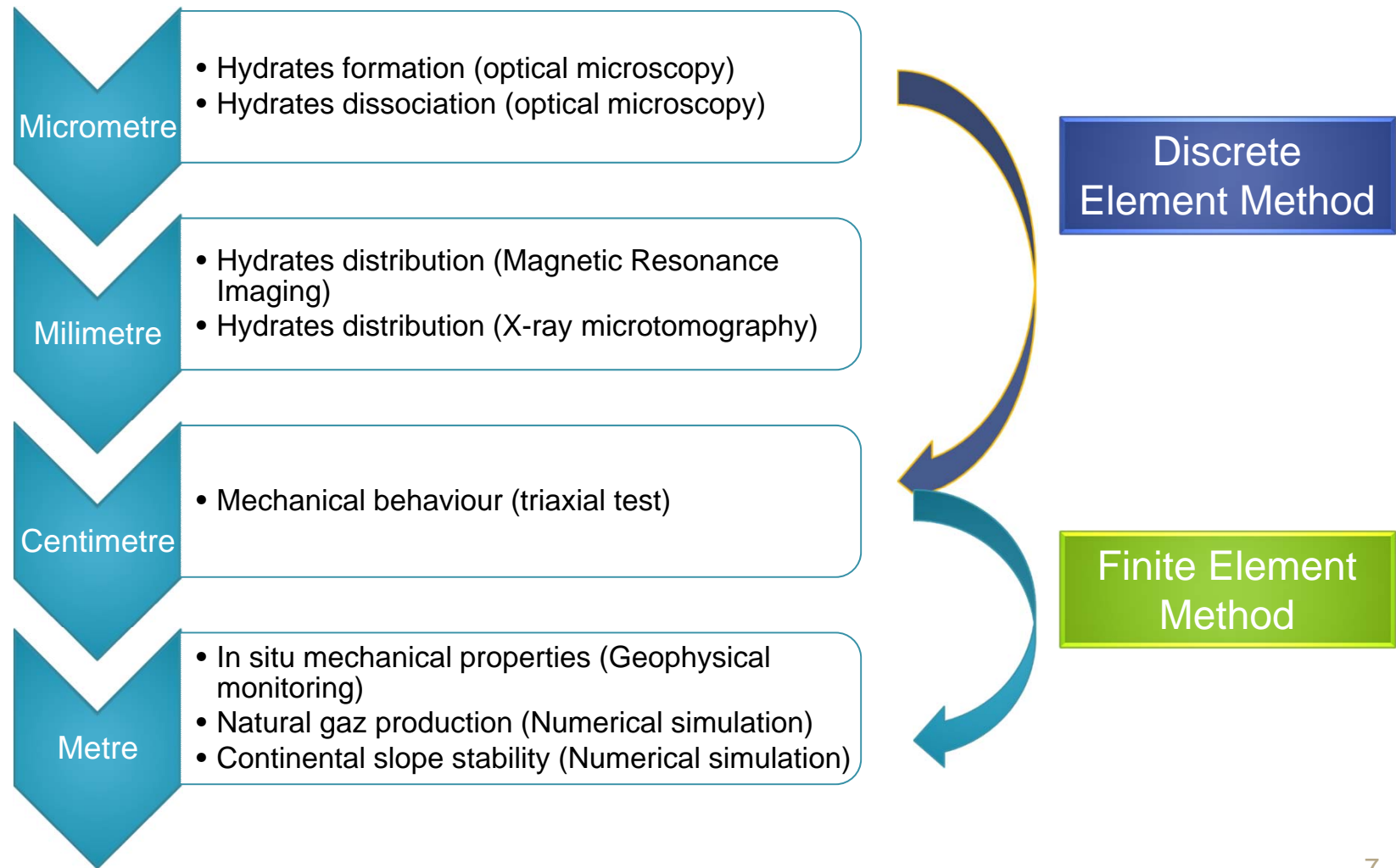
India: <http://www.dghindia.org/NonConventionalEnergy.aspx>

UNEP Report: <http://www.methanegashydrates.org/>

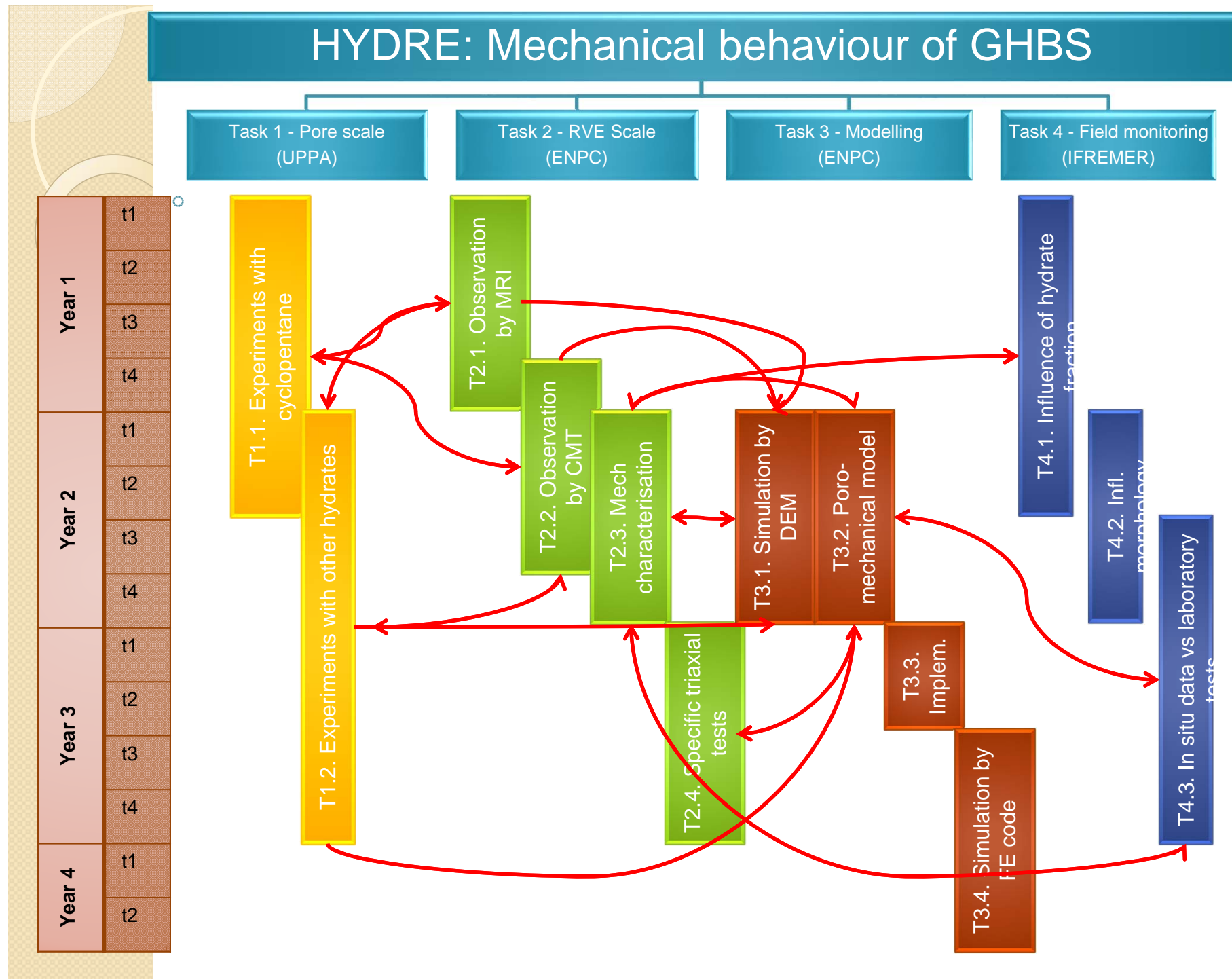
Journal "Fire in the Ice": <http://www.netl.doe.gov/research/oil-and-gas/methane-hydrates/fire-in-the-ice>

World Ocean Review: <http://worldoceanreview.com/en/wor-3-overview/methane->

Programme scientifique



HYDRE: Mechanical behaviour of GHBS

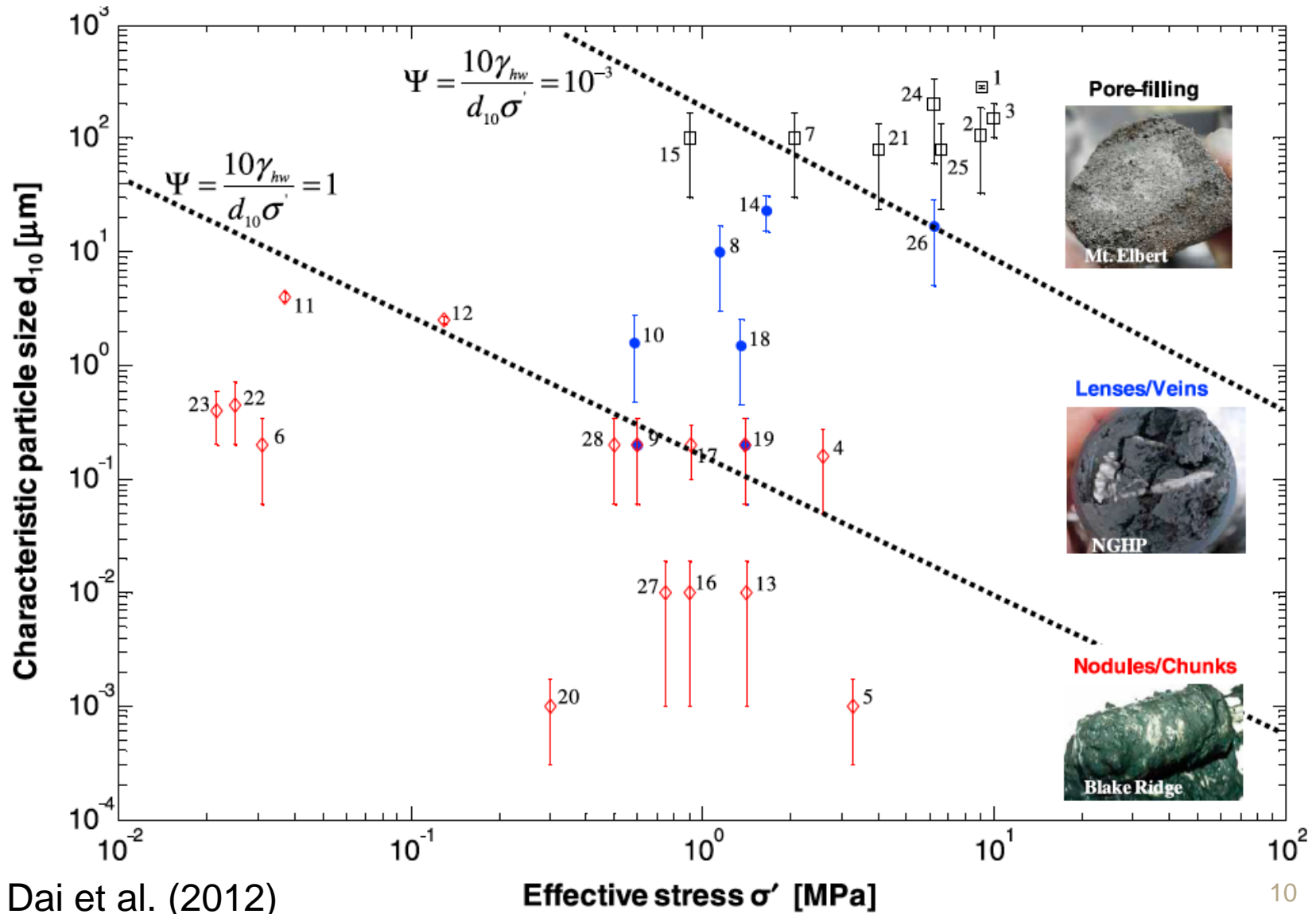


Morphologie

Location	No.	Depth ^b (m)	Water Depth (m)	Hydrate Morphology	Sediment Description	Index Properties ^c			Typical Values
							Mean	s.dev.	
Mallik	1	913.7	913.7	pore filling	granular/pebbles (max 1 cm)	$d_{10} = 275.9\text{--}292.9 \mu\text{m}$ (at 912.3 m)	285	8.5	fine/medium sands: 0.06–0.6 mm
	2	903	903	pore filling	medium-grained sand	$d_{10} = 108.4 \mu\text{m}$ (at 908.3 m)	108.4	76.02	
	3	892.8–1088.1	990.45	pore filling	medium/fine sands	$d_{50} = 149.9\text{--}502.5 \mu\text{m}$	150	50	
Blake Ridge	4	259	3058.1	nodules	nano fossil-rich clay	$d_{50} = 1.6 \mu\text{m}$	0.16	0.11	Smectite: ~1 nm Kaolinite: ~0.1–1 μm
	5	330	3100.1	chunks	55% Illite + 45% Smectite		0.001	0.0007	
	6	3.09	2781.59	nodules/chunks	soft clay (39.2% clay)	LL = 68; PL = 24	0.2	0.14	
Nankai Trough	7	207.8–260	1178.9	pore filling	sandy sediments		100	70.13	fine/medium sands: 0.06–0.6 mm silt: 2–60 μm Kaolinite: ~0.1–1 μm
	8	90–140	4799.3	veins	60% sand/granules + 40% silt		10	7.01	
	9	60	1300	veins (nodules?)	fine grained clay minerals	$S_s = 87\text{--}94 \text{ m}^2/\text{g};$ $LL = 73\text{--}75;$ $PL = 34\text{--}36$	0.2	0.14	
NGHP	10	58.44	1107.44	veins		$\phi_{10} = 9.28; \phi_{50} = 6.08$	1.6	1.12	Illite: ~10–100 nm
	11	3.7	678.2	nodules	soft clay sediments	$\phi_{50} = 5.7; S = 1.2;$ $Sk = -0.81$ (at 3.59 m)	4	0.3	
	12	13.05	687.55	nodules		$\phi_{50} = 4.05; S = 0.95;$ $Sk = -0.58$	2.5	0.2	
Offshore Peru	13	141	3961	nodules	diatomaceous muds (44% Illite)		0.01	0.01	Illite: ~10–100 nm
	14	165.6	5235.6	nodules	diatomaceous muds	$\phi_{10} = 5\text{--}6$	23	8	
	15	88.3–97.9	2715.7	pore filling	Sandy sediments		100	70.13	
Okushiri Ridge	16	88.3–97.9	2715.7	nodule	diatom-bearing clays, silty clay	$LL = 113\text{--}143$ (at 83.75–189.9 m, 799A)	0.01	0.01	Illite: ~10–100 nm
	17	91.07	2661.67	nodule	abundant diatoms	75% sand + 15% silt + 10% clay	0.2	0.1	
	18	136	2100	veins/lenses	microfossile, clay	$d_{50} = 3.041 \mu\text{m}; d_{10} = 1.5 \mu\text{m}$	1.5	1.05	
Orca Basin, GOM	19	140	2218	vein and nodule		18% clay + 82% silt $S_s = 71$ (at 141 m)	0.2	0.14	Kaolinite: ~0.1–1 μm Smectite ~1 nm fine sands: 60–200 μm
	20	20–40	2425	nodules	smectite dominant clay	$LL = 83; PL = 31$	0.001	0.0007	
	21	~400	~3130	pore filling	fine sands		80	56.10	
Alaminos Canyon, GOM Sea of Okhotsk	22	2.3–2.7	~840	nodules	20.42% clay	$\phi_{50} = 6.13; S = 1.73;$ $Sk = 1.4; Kt = 2.16$	0.45	0.25	
	23	1.65–2.65	~670	nodules/veins	23.4% clay	$\phi_{50} = 6.35; S = 1.70;$ $Sk = 1.31; Kt = 2.09$	0.4	0.2	
	24	619.9	619.9	pore filling	fine quartz sand	$d_{10} = \sim 0.2 \text{ mm}$ (at 618.1 m)	200	140.26	
Mt. Elbert	25	661	661	pore filling	fine-grained quartz	$d_{10} = \sim 0.08 \text{ mm}$ (at 662.4 m)	80	56.10	
	26	620	620	vein	silty sand	$d_{10} = 0.017 \text{ mm}$	17	11.92	



Morphologie



Formation d'hydrates en laboratoire

03

Waite et al.: PHYSICAL PROPERTIES OF HYDRATE-BEARING SEDIMENTS

I

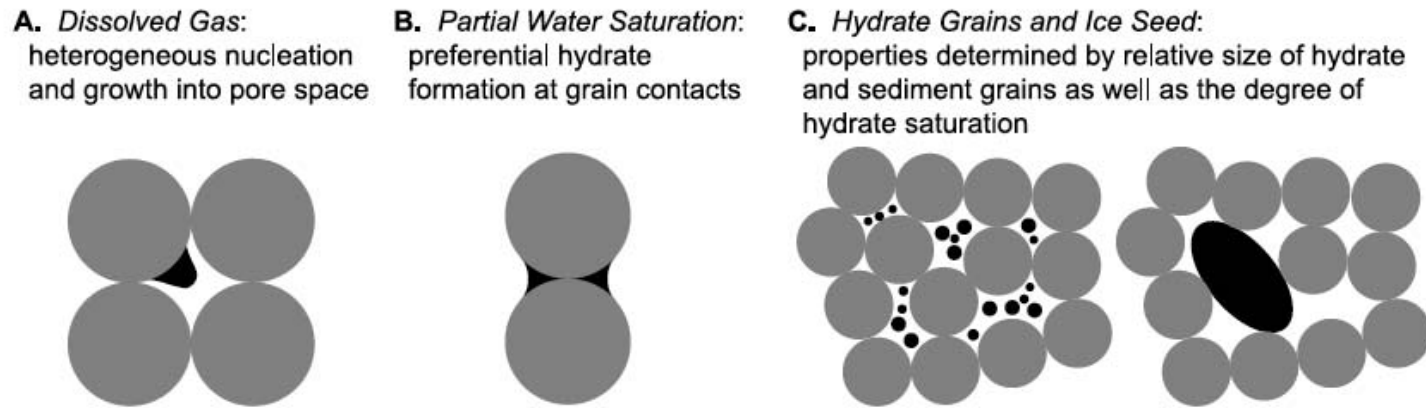
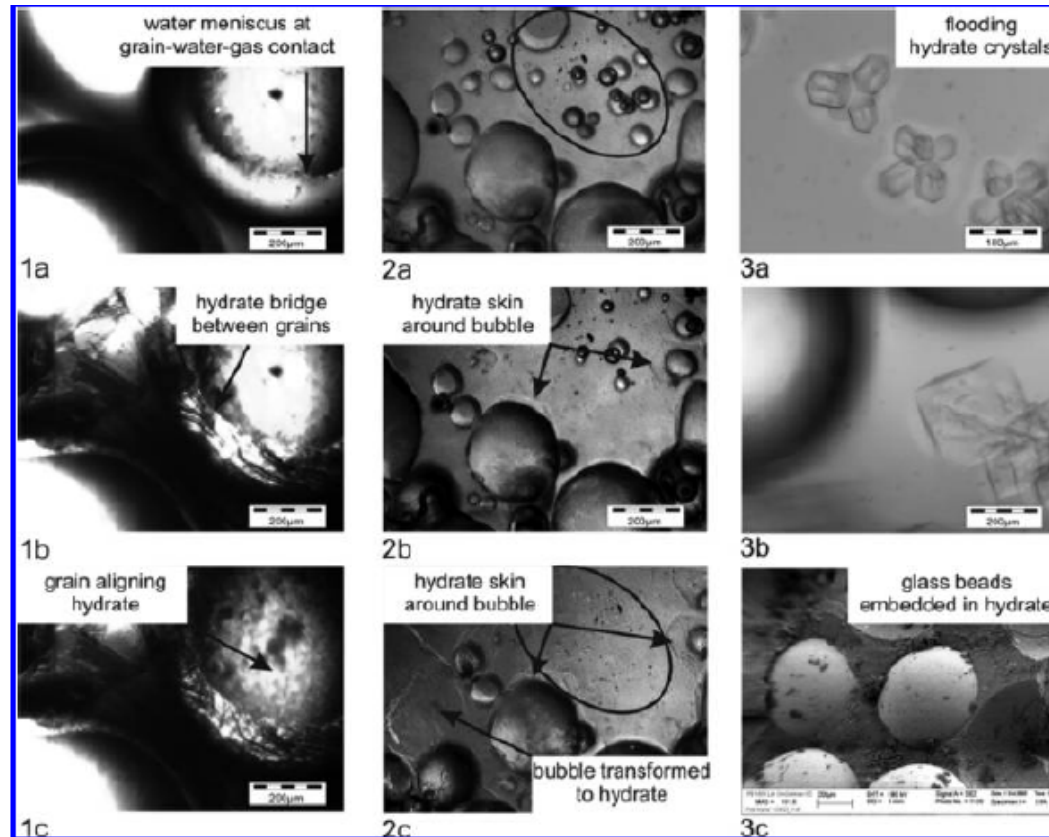


Figure 3. Dependence of hydrate habit on hydrate formation technique. Physical properties of hydrate-bearing sediments depend on the size and distribution of hydrate (black) relative to the sediment grains (gray).

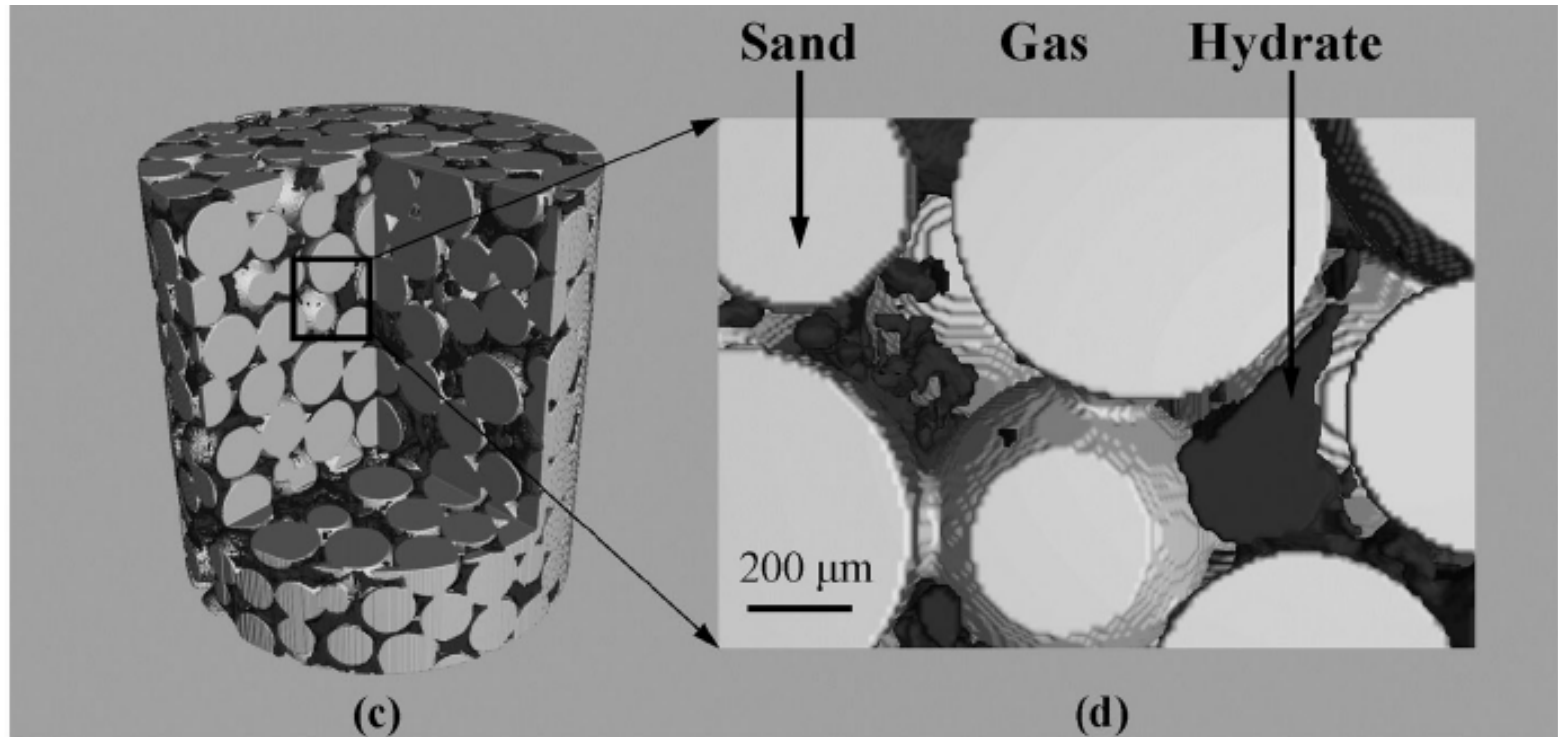
Microscopie



Spangenberg et al., 2015

Figure 4. Images of hydrate growing from water and free methane gas (panels 1 and 2) and from methane dissolved in water (panels 3). The procedure to gain these photographs is described in detail in Spangenberg et al.¹⁷ (1a) Glass beads, water, and methane situated outside the hydrate stability. (1b) Hydrate growing at the gas–water interface forming a bridge between neighboring grains. (1c) Water, wetting the glass beads is finally transformed into hydrate and the grain surface is covered with grain aligning hydrate. (2a) Methane bubbles in water outside the hydrate stability field. (2b) Within the hydrate stability field hydrate starts to form around the bubbles. (2c) Large bubbles are transformed to hydrate (some with a gas inclusion inside), whereas smaller bubbles disappear due to dissolution and hydrate formation (see ellipse in panels 2a and 2b). (3a) Hydrate formed from methane dissolved in water without a free-gas phase crystallizes in the pore water. (3b) To date there is no evidence that hydrate crystals grow at grain surfaces. We could only observe hydrate flooding in the pore water. (3c) An SEM-image of glass beads embedded in a matrix of almost pure methane hydrate (ice to hydrate ratio is 17 % to 83 %).¹⁵

Microtomograph aux rayons X



IRM

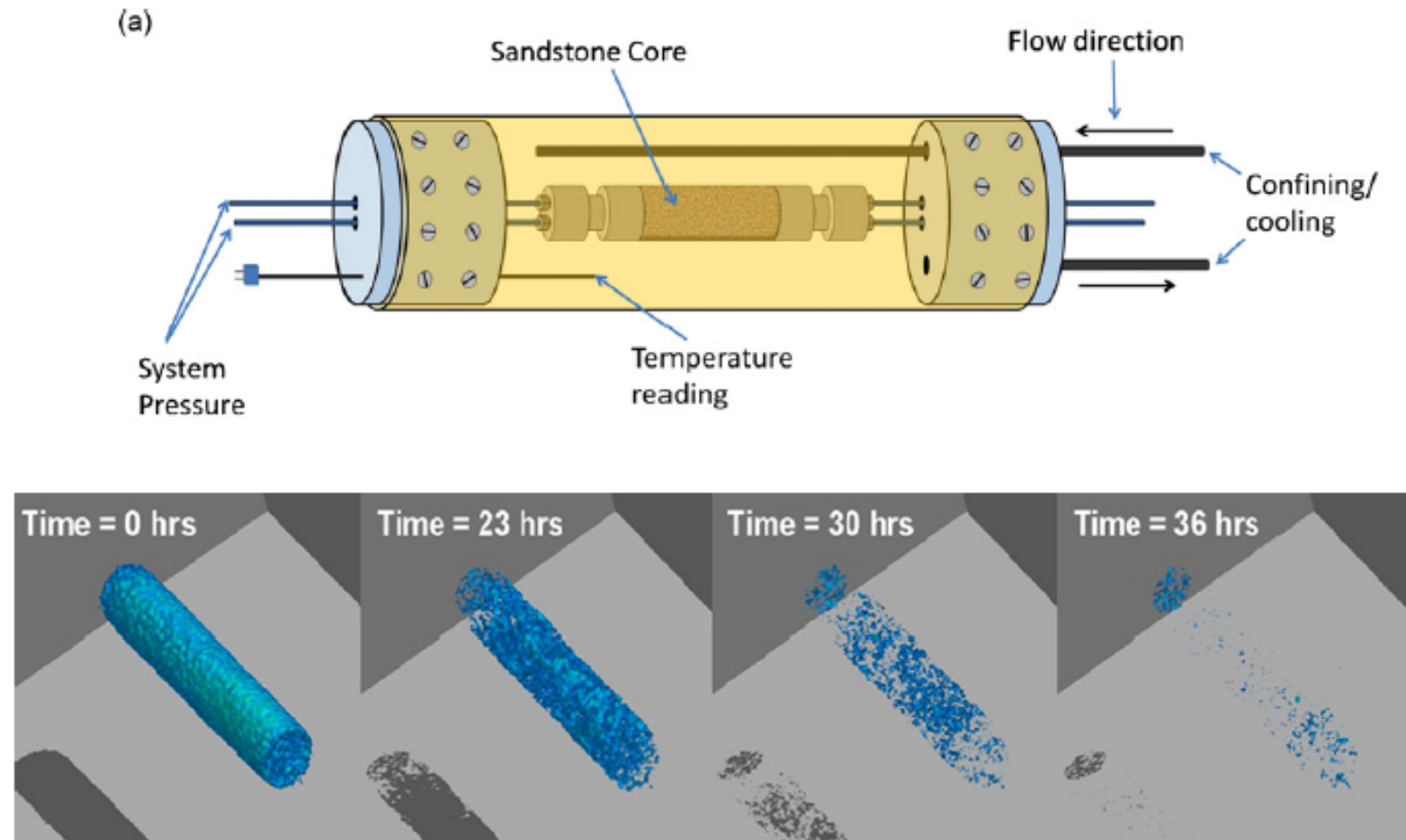
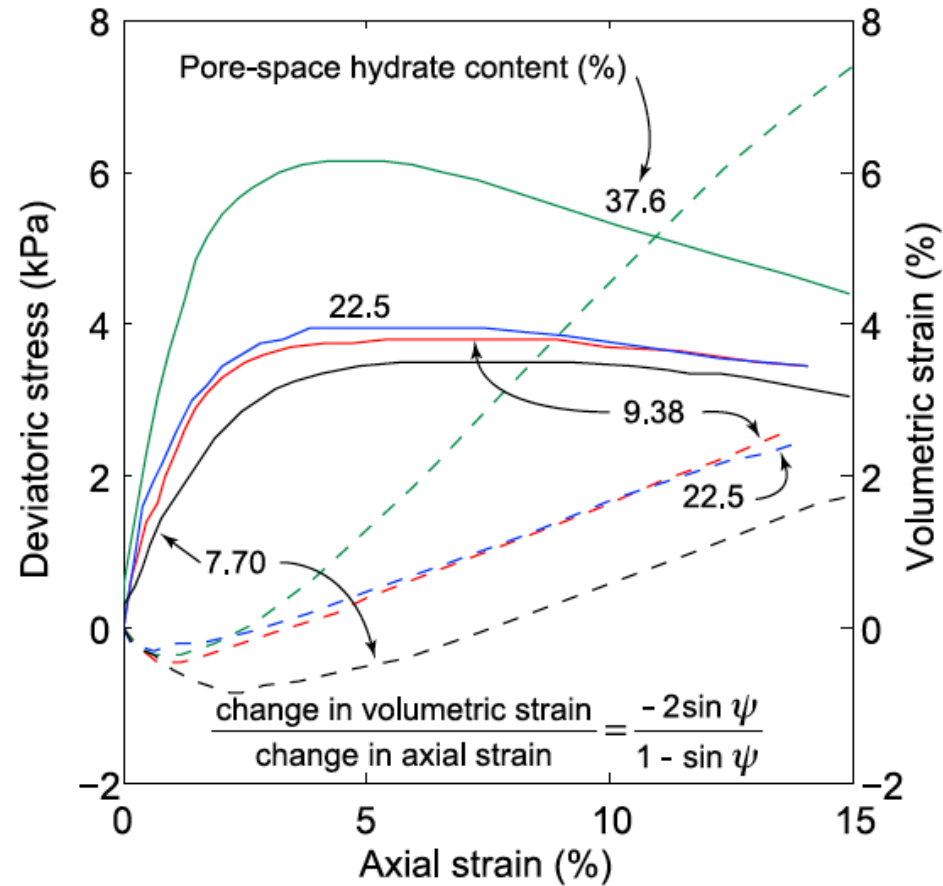


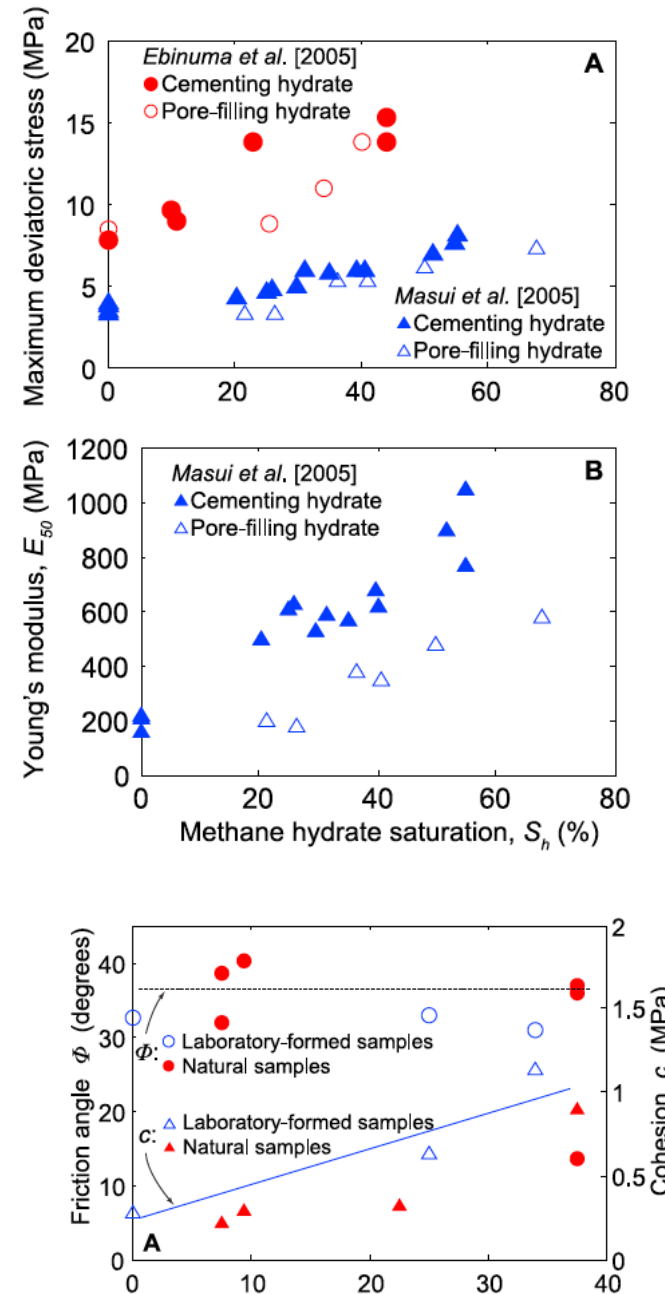
Fig. 4. Hydrate formation in whole core [3].



Essai triaxial



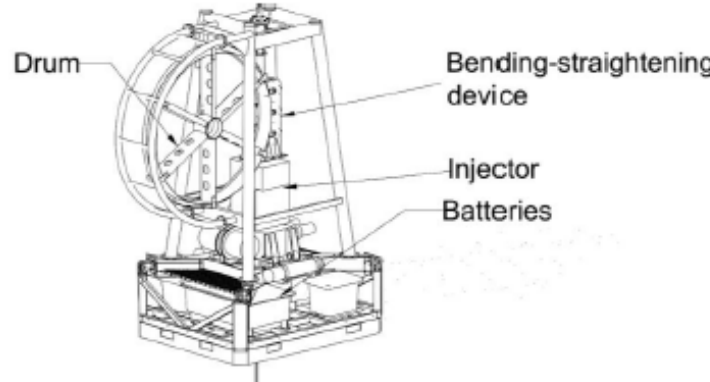
Waite et al (2009)



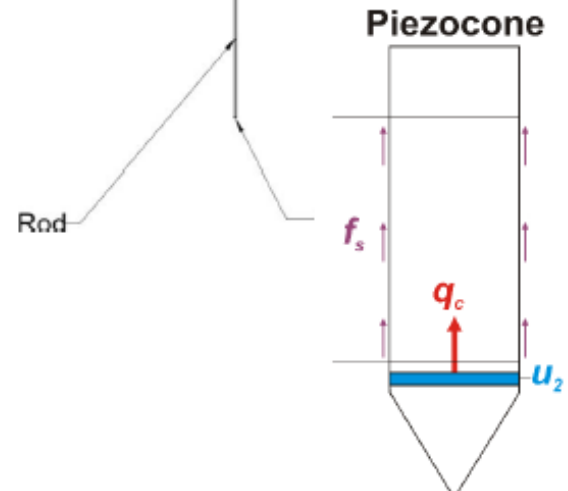


Measures in situ

Penfeld penetrometer



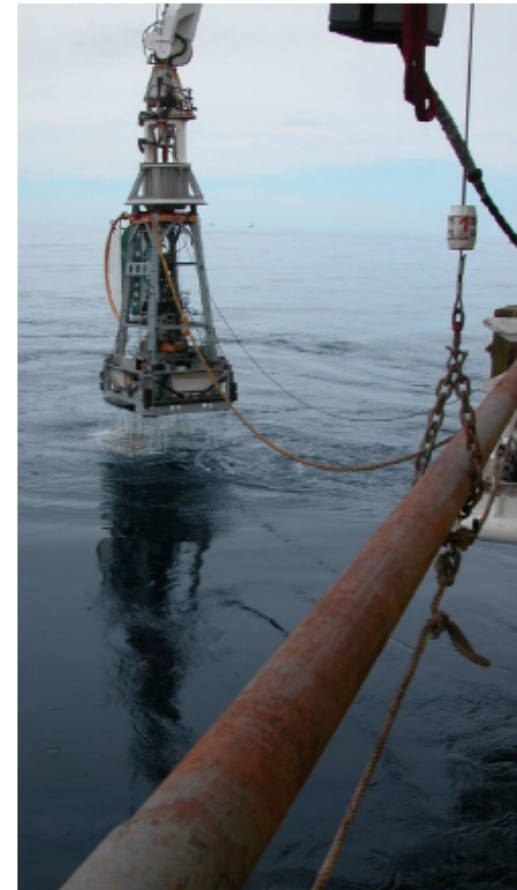
Piezocene



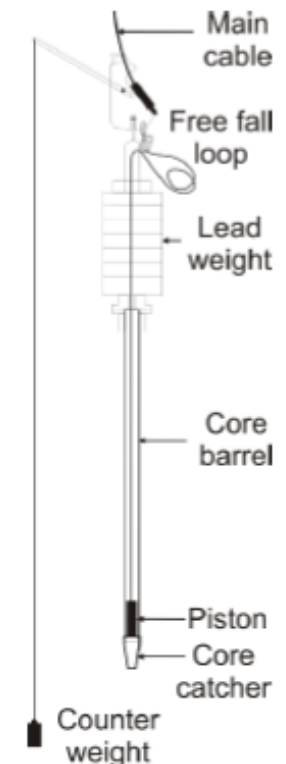
q_c : Tip resistance

f_s : Friction Sleeve

u_2 : Pore pressure



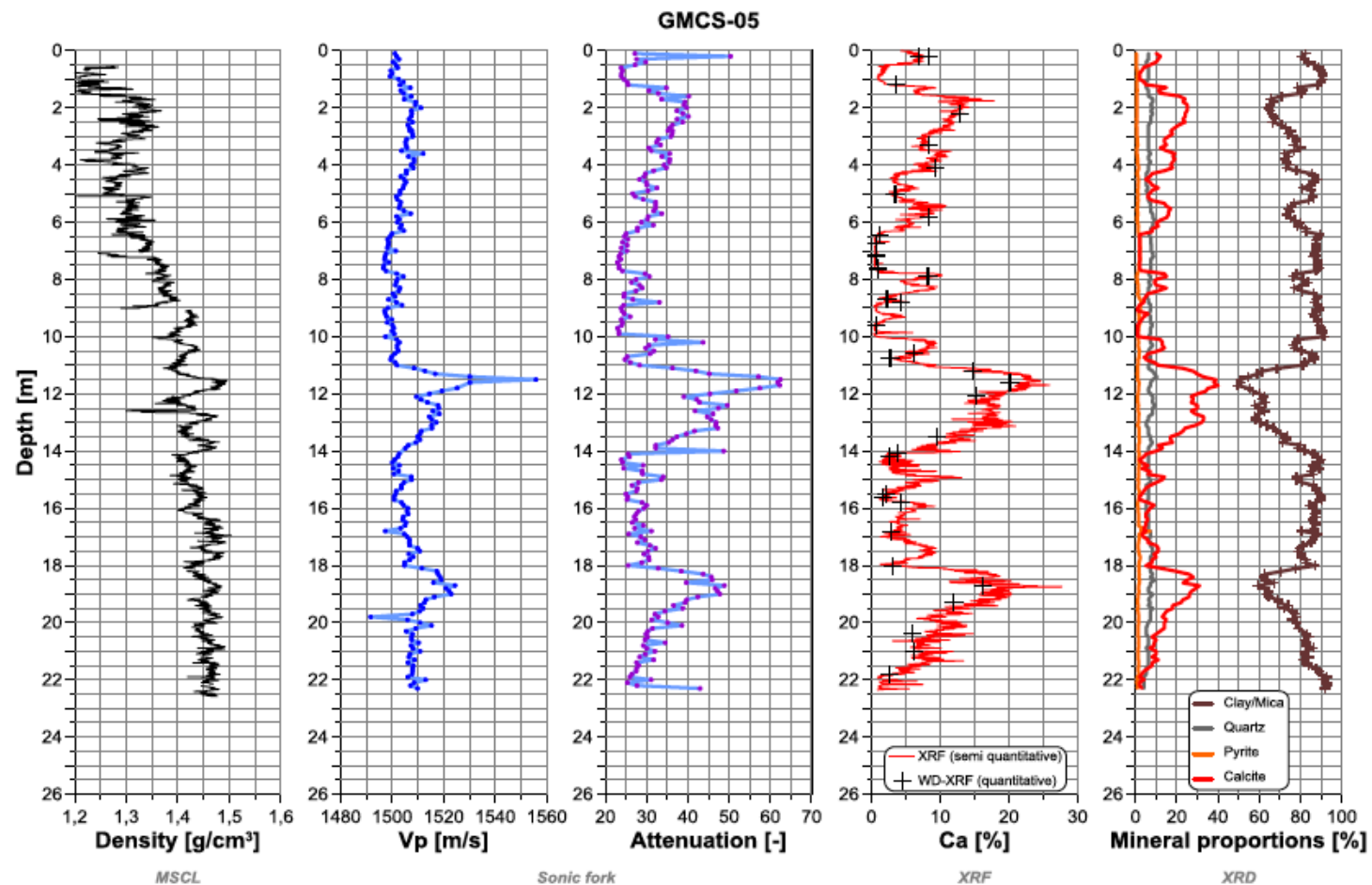
Calypso piston corer





Mesures in situ vs laboratoire

Analyse de mesures in situ et en laboratoire pour déterminer la quantité d'hydrates de gaz



Etablir un modèle pétrophysique

Modélisation par éléments discrets

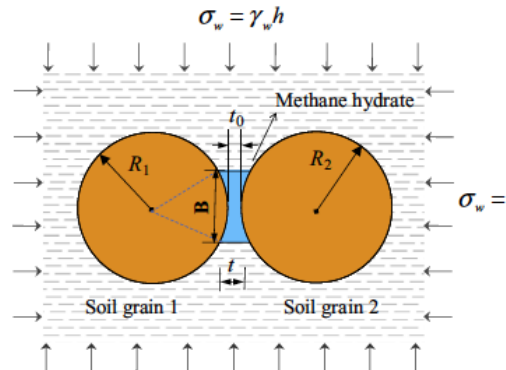
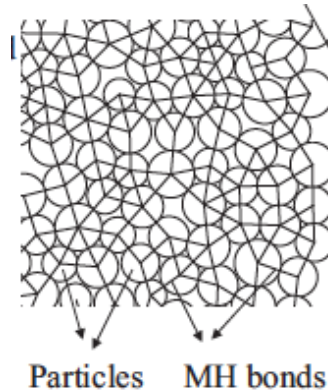
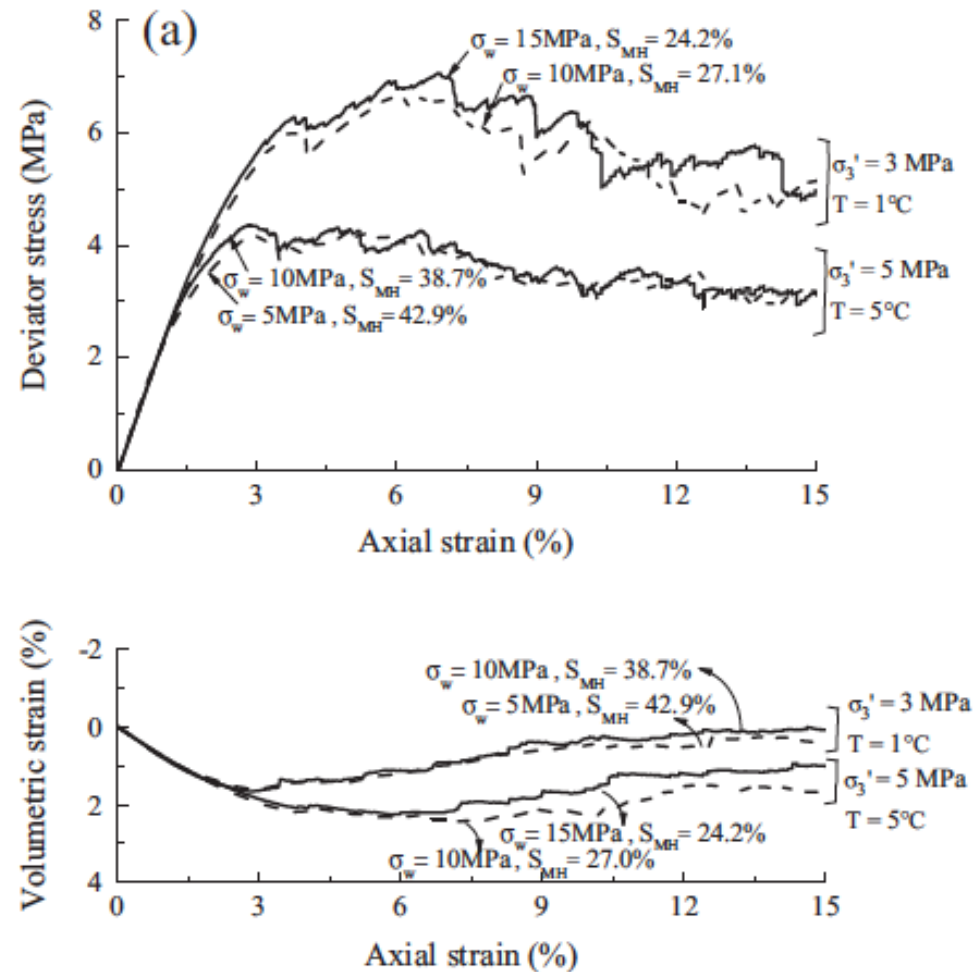


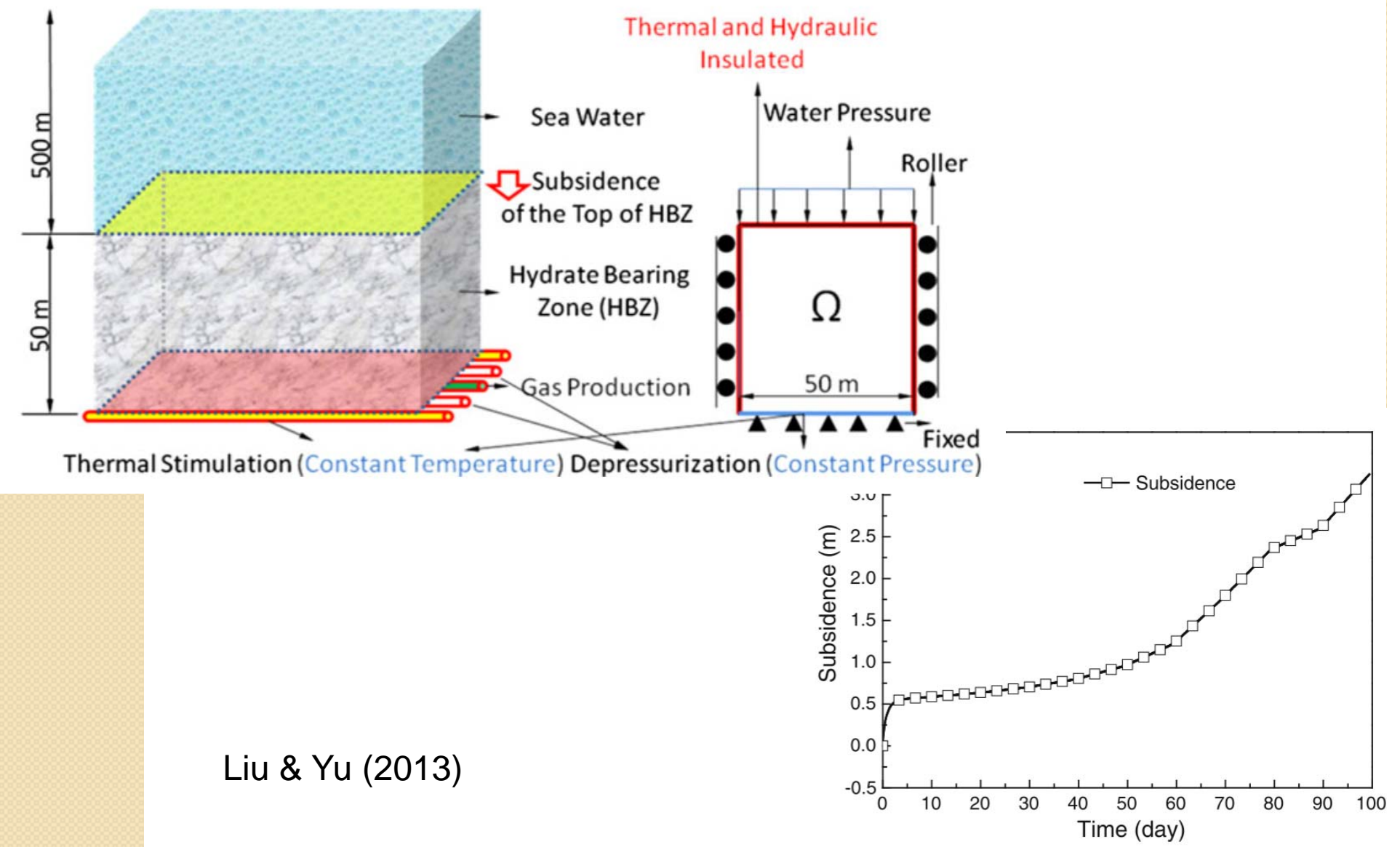
Fig. 3. A pair of soil grains immersed in water and cemented b



Jiang et al (2015)



Modélisation par éléments finis





Retombées attendues

- **Scientifiques:** Formation/dissociation hydrates; Effet des hydrates; Détection in situ; Appréhension de risques; Publications, séminaire.
- **Techniques:** Observations optiques; Système de contrôle de température/pression pour dispositifs existants; Modèles constitutifs macroscopiques; Code de calcul numérique; Méthode de mesure in situ; Gestion de projet.
- **Economiques:** Avancées dans l'exploitation des hydrates de gaz comme sources d'énergie; Stockage CO₂ (formation des hydrates de CO₂); Prédiction du dégagement de gaz à effet de serre (dissociation des hydrates; Autres domaines technologiques basés sur les hydrates)

Participants

Partner	Surname	First name	Role and sphere of responsibility for the project
ENPC	TANG	Anh Minh	<i>Thermo-hydro-mechanical experiments</i>
UPPA	BROSETA	Daniel	<i>Formation and dissociation of gas hydrates at the pore scale</i>
ENPC	PEREIRA	Jean-Michel	<i>Numerical modelling by Finite Element Method</i>
IFREMER	GARZIGLIA	Sebastien	<i>Analysis of in situ data</i>
UPPA	BOURIAT	Patrick	<i>Emulsion and colloidal behaviour</i>
UPPA	BROWN	Ross	<i>Optical microscopy</i>
ENPC	BORNERT	Michel	<i>X-ray micro-tomography</i>
ENPC	AIMEDIEU	Patrick	<i>X-ray micro-tomography</i>
ENPC	RODTS	Stéphane	<i>Magnetic Resonance Imaging</i>
ENPC	ROUX	Jean-Noël	<i>Discrete Element Method</i>
ENPC	DANGLA	Patrick	<i>Physicochemical couplings in porous media</i>
IFREMER	SULTAN	Nabil	<i>Analysis of in situ data</i>

Merci de votre attention!

Anh Minh TANG

Ecole des Ponts ParisTech

anhminh.tang@enpc.fr